Chemical State Mapping of Degraded B4C Control Rod Investigated with Soft X-ray Emission Spectrometer in Electron Probe Micro-analysis.

AUTHOR(S):

Kasada, R; Ha, Y; Higuchi, T; Sakamoto, K

CITATION:

Kasada, R ...[et al]. Chemical State Mapping of Degraded B4C Control Rod Investigated with Soft X-ray Emission Spectrometer in Electron Probe Micro-analysis.. Scientific reports 2016, 6: 25700.

ISSUE DATE:

2016-05-10

URL:

http://hdl.handle.net/2433/212046

SCIENTIFIC REPORTS

OPEN

Received: 04 January 2016
Accepted: 21 April 2016
Published: 10 May 2016

Chemical State Mapping of Degraded B_4C Control Rod Investigated with Soft X-ray Emission Spectrometer in Electron Probe Micro-analysis

R. Kasada[1], Y. Ha[1], T. Higuchi[2] & K. Sakamoto[2]

B_4C is widely used as control rods in light water reactors, such as the Fukushima Daiichi nuclear power plant, because it shows excellent neutron absorption and has a high melting point. However, B_4C can melt at lower temperatures owing to eutectic interactions with stainless steel and can even evaporate by reacting with high-temperature steam under severe accident conditions. To reduce the risk of recriticality, a precise understanding of the location and chemical state of B in the melt core is necessary. Here we show that a novel soft X-ray emission spectrometer in electron probe microanalysis can help to obtain a chemical state map of B in a modeled control rod after a high-temperature steam oxidation test.

Control rods used in boiled-water reactors (BWRs) in Japan, including all units at the Fukushima Daiichi nuclear power plant (NPP), consist of stainless steel tubes filled with B_4C granules[1]. B_4C is stable at the normal NPP operating temperature of ~300 °C, as it melts at 2450 °C[2]. However, the eutectic interaction of B_4C with the adjacent stainless steel leads to its liquefaction at temperatures exceeding 1200 °C under severe accidental conditions[1–5]. The appearance of this liquid phase causes the phenomenon of candling and relocation, in which the liquid phase sinks to the bottom of the nuclear core. The proper pouring of cooling water is necessary to prevent achieving recriticality when B is not available as a neutron absorber at the upper part of the core. In addition, the oxidation of B_4C by high-temperature steam may first form B_2O_3 and then gaseous boric acids (HBO_2 and H_3BO_4)[3]. The release of these gases may affect the source term of radioactive materials. Therefore, the prediction and evaluation of B and the chemical state thereof is necessary to control accidents.

The spatial distribution of B in B_4C after severe accidental simulation tests has been analyzed mainly by scanning electron microscopy (SEM) with energy-dispersive X-ray spectroscopy (EDS) and by electron probe microanalysis (EPMA) with wavelength-dispersive X-ray spectroscopy (WDS)[1,5]. However, these conventional methods do not easily provide chemical state information, as they are limited by insufficient energy resolution. Although soft X-ray emission or absorption spectrometry, using synchrotron radiation facilities, may provide an understanding of the chemical state of B[6,7], it is not economically viable to simultaneously obtain a detailed spatial distribution.

In this study, we demonstrate the chemical state mapping of B in a modeled B_4C control rod after a high-temperature steam oxidation test using the newly developed EPMA-soft X-ray emission spectrometer (SXES) with ultra-high energy resolutions[8,9]. EPMA-SXES is a type of WDS that performs a parallel collection of soft X-ray spectra by a combination of an aberration-corrected grating system and a high-sensitivity X-ray charge-coupled device (CCD). Therefore, EPMA-SXES permits the spectral mapping of light elements.

Results and Discussion

Figure 1 shows the soft X-ray emission spectra of B-Kα from B-containing crystalline materials such as (a) B_2O_3, (b) B, (c) B_4C, (d) Fe_2B, and (e) FeB as references for EPMA-SXES. The spectra were normalized by the maximum

[1]Institute of Advanced Energy, Kyoto University, Gokasho, Uji, Kyoto 611-0011, Japan. [2]Nippon Nuclear Fuel Development, Co., Ltd., 2163 Narita-cho, Oarai, Ibaraki 311–1313, Japan. Correspondence and requests for materials should be addressed to R.K. (email: r-kasada@iae.kyoto-u.ac.jp)

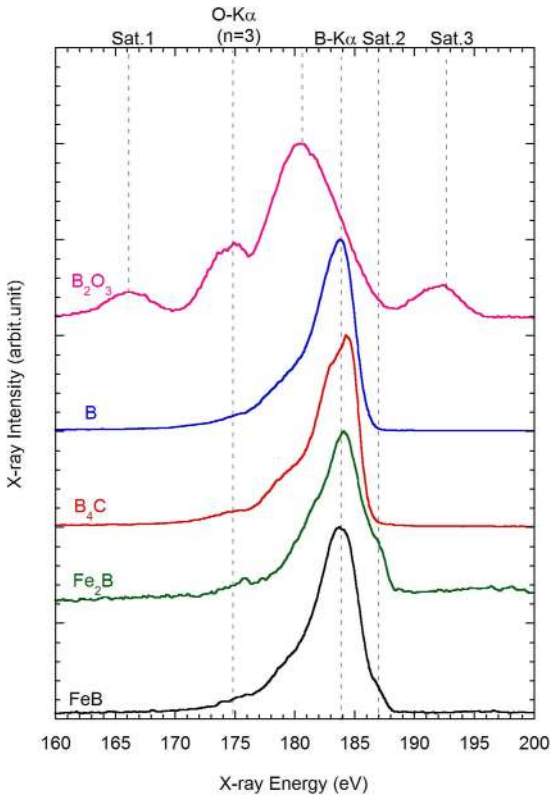

Figure 1. Soft X-ray emission spectra from B_2O_3, B, B_4C, Fe_2B, and FeB, obtained by EPMA-SXES.

intensity of each B-Kα peak. As reported in the Handbook of X-Ray Data[10], the B-Kα peak is observed at 183.5 eV for B. The B-Kα peak of B_4C shifts to a slightly higher energy at 184 eV and shows a characteristic shape with decreased intensity at lower-energy. The change in the spectral shape is attributed to the bonding of B and C within B_4C. The spectra of the iron borides FeB and Fe_2B depict clear shoulders, designated as Sat.2 in the upper horizontal axis of Fig. 1, near 187 eV. These shoulders relate to the Fermi level of the material, as the electron behavior of B in iron borides is more metallic than that in the pure element[11]. The shoulders may also relate to the slightly higher energy of the peak of Fe_2B than those of B and FeB. Notably, B_2O_3 shows a distinctly different spectral shape compared to that of the other B-containing materials. The B-Kα peak of B_2O_3 experiences a large shift to a lower energy at 180.5 eV and the formation of two additional satellite peaks: one higher (Sat.3: 192.5 eV) and one lower (Sat.1: 166 eV). Muramatsu *et al.* revealed that the higher-energy satellite peak originated from resonant X-ray Raman scattering and linked the lower-energy satellite peak to a transition from the B 2*p* and O 2*s* molecular orbitals to a core hole at the B 1*s* orbital[12]. Thus, we consider that EPMA-SXES has a sufficiently high energy resolution to determine the chemical state of B from the changes in the spectral shape of the B-Kα peak.

Figure 2 shows (a–g) elemental mapping results obtained by conventional EPMA-WDS, (h) a secondary electron image, and (i) a back-scattering electron image on the cross-section of the B_4C control rod model after exposure to high-temperature steam at 1250 °C for 30 min. Although B_4C and stainless steel reacted significantly, B_4C granules remain in the red- and pink-colored region in the (d) B map. Alloying elements of stainless steel such as Fe, Cr, and Ni are observed within the stainless tube where the B_4C granules were placed before the oxidation test. Because these area also contains some amounts of B, liquefaction by eutectic interactions between B_4C and stainless steel occurs under the high-temperature oxidation testing condition; the liquid solidifies as the test temperature is decreased. The electron images (h,i) show that the peripheral vicinity of the remaining B_4C granule comprises a layer of reaction products from B_4C with stainless steel and/or steam. The elemental maps show that the peripheral vicinity of the remaining B_4C contains relatively dense O and C. The chemical state information of B will determine whether these are from B_2O_3 formed by the oxidation of B_4C or from other oxides.

In Fig. 3, we show the EPMA-SXES measurement result of (a–c) a B elemental map for the same position as Fig. 2 and (d) B-Kα spectra from the points A through K, as designated in the elemental map. The B-Kα spectra (solid lines) for the points of the remaining B_4C granule present the characteristic peak shape of B_4C, as shown in Fig. 1. However, the B-Kα spectra (dotted lines) for the points farther from the remaining B_4C granule exhibit a unique shoulder at ~187 eV, similar to the shoulders in the spectra of the iron borides. Thus, EPMA-SXES supports that B in B_4C reacts with the stainless steel to form borides. Although the peak of O-Kα (n = 3) is also observed near the B_4C particle, the shape of the B-Kα peak differs from that of B_2O_3. Therefore, the O near the B_4C granule probably results from other metal oxides.

To understand the reaction process of the B_4C control rod model after high-temperature steam oxidation testing, it is beneficial to visualize the chemical distribution of B in the model. To clarify the chemical state, the

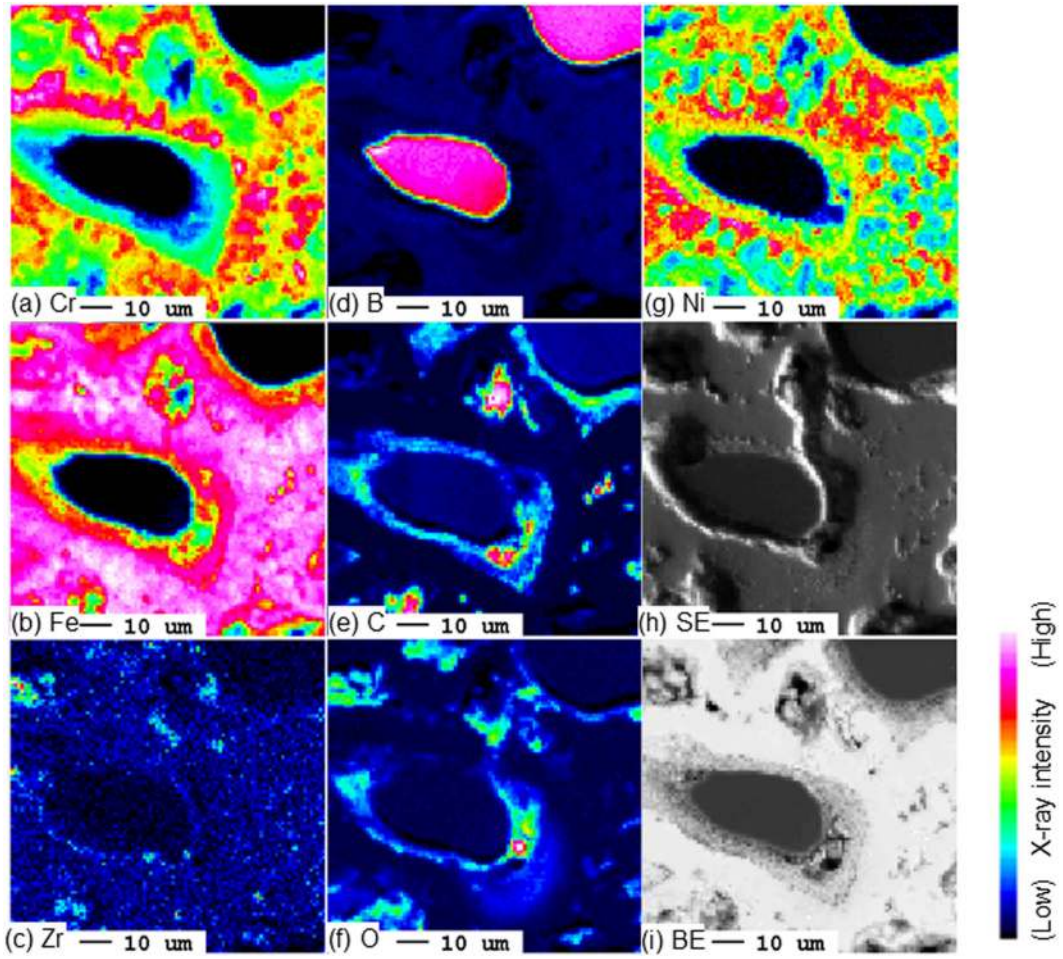

Figure 2. Elemental mapping and scanning electron images obtained by EPMA-WDS on the cross-section of B_4C control rod after high-temperature steam oxidation test at 1250 °C for 30 min.

elemental maps shown in Fig. 3(a–c) are re-calculated by the areal ratios of the peaks; P_A is the total area of B-Kα in the range 178–188 eV, P_B is the area from 178 to 186 eV, and P_C is the area in 186–188 eV. Figure 3(e,f) show the chemical state maps obtained by calculating P_B/P_A and P_C/P_A, which display the existing areas of B_4C and borides separately.

Thus, we succeeded in identifying the chemical state of B and in visualizing the spatial distribution of B with associated chemical states in the degraded B_4C control rod model, based on EPMA-SXES with ultrahigh energy resolution. Our findings will aid the establishment of severe accident simulation codes and the prediction of the chemical state and physical location of B in the Fukushima Daiichi NPP. In addition, we emphasize that the present lab-scale SXES by EPMA has excellent energy-resolution and higher spatial resolution not only for light elements but also for higher atomic number elements compared with SXES by synchrotron radiation facilities. EPMA-SXES permits the visualization of the chemical state of elements in various materials at the micro-scale.

Methods

Reference materials. Five B-containing crystalline materials were prepared; B granules (3–7 mm) and B_2O_3 powder were purchased from Kojundo Chemical Laboratory Co., Ltd. FeB and Fe_2B (500 μm in diameter) were purchased from Goodfellow Cambridge Ltd. B_4C granules were supplied by a domestic BWR manufacturer in Japan. The chemical compositions were shown elsewhere[7].

High-temperature steam oxidation test. We used a control rod model containing B_4C granules[7] as neutron absorbers, SUS304L as cladding tube, SUS316L as control rod blade, and Zircaloy-4 as the channel box material as shown in Fig. 4. The B_4C granules were placed in the cladding tubes, which are 0.6 mm in thickness, 4.8 mm in outer diameter and 20 mm in length. The vibration method was used for filling B_4C granules with a packing density of approximately 70%. Then the ends of the tubes were sealed with setscrews of SUS304. Three sets of stainless steel tubes filled with B_4C were sandwiched by the control rod blade material (SUS316L) and the channel box material (Zircaloy-4), which was coated with an oxide film of approximately 20 μm in thickness on the surface, equivalent to that formed on the actual component by exposure to water vapor at 1000 °C for 10 min.

The high-temperature steam oxidation test was performed on the model for 30 min at 1250 °C, at which point the eutectic interaction of B_4C and stainless steel is known to be rapid. The heating of the model was performed

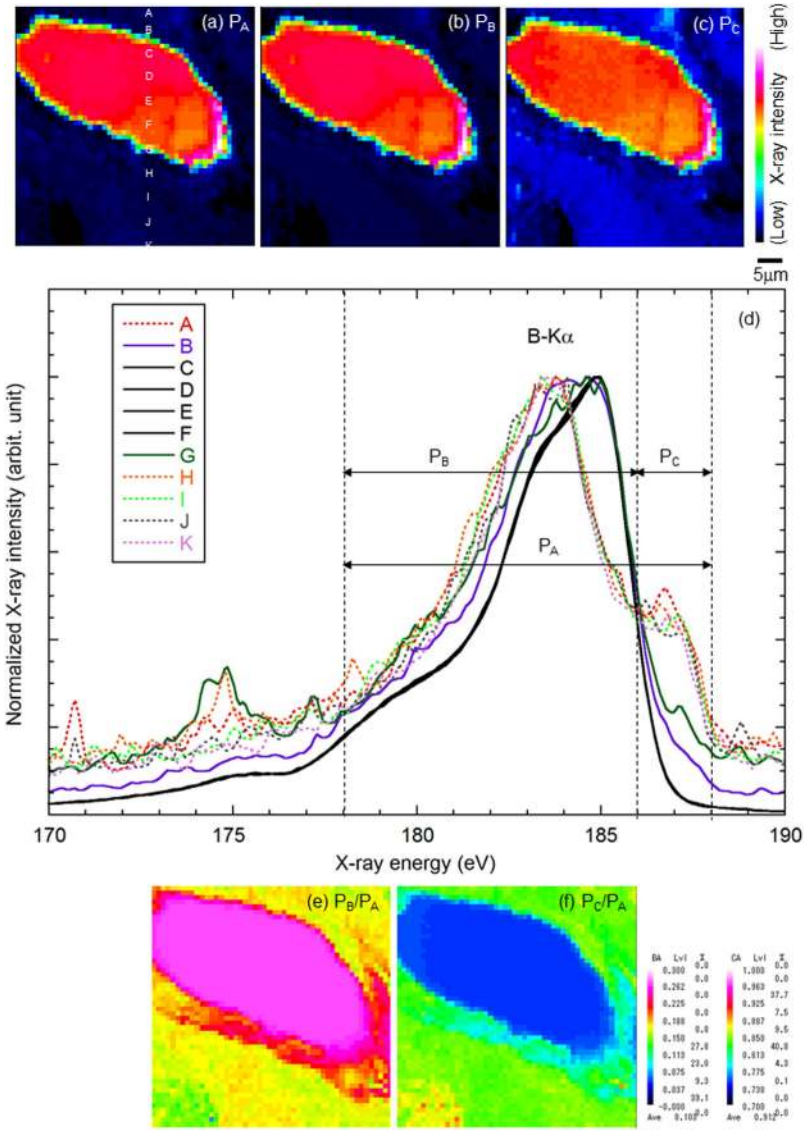

Figure 3. Elemental maps based on (**a**) P_A, (**b**) P_B, and (**c**) P_C of (**d**) B-Kα spectrum, obtained by EPMA-SXES and re-calculated by peak-area ratio as (**e**) P_B/P_A and (**f**) P_C/P_A.

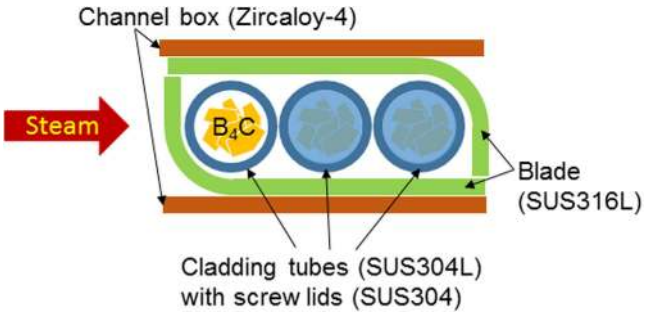

Figure 4. Schematic of the B_4C control rod model used.

by a horizontal electric furnace using a KERAMAX ($LaCrO_3$) heater. Firstly, the model was set on a sample table located in a low-temperature part of the reaction tube. Secondly, the furnace was kept at the target temperature under flowing humidified Ar gas. Thirdly, the sample table was moved into the high-temperature part of the reaction tube using a heat-resistant push rod. After 30 min in this region, the test was completed by transferring the

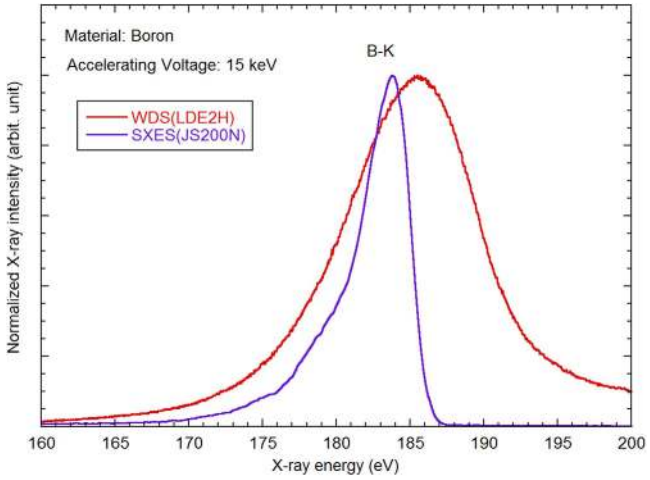

Figure 5. Comparison of B-Kα spectra obtained by EPMA-WDS using LDE2H and EPMA-SXES using JS200N as spectrometer.

sample stage, using the push bar, to the opposite low-temperature region. The Ar gas was humidified by bubbling the Ar at 800 cm^3/min into a constant-temperature water bath kept at 70 °C.

After the high-temperature steam oxidation test, the model was cut at the axial direction center position and embedded into resin. The cross-section was polished with SiC papers and colloidal silica. The final surface of the cross-section was Pt-coated to prevent charge-up.

EPMA-WDS and SXES. The polished sample was examined by a JXA-8500F field emission EPMA (JEOL) equipped with WDS and SXES. The acceleration voltage and beam current of the scanning electron beam were 15 keV and 5.5×10^{-7} A, respectively. The energy range of SXES was 54 to 220 eV. The nominal energy resolution for SXES was 0.22 eV. Figure 5 shows the soft X-ray emission spectra of B-Kα from B granules obtained by a conventional WDS (type LDE2H) and the newly developed SXES (type JS200N). The advantages of SXES in energy resolution are evident. The broad asymmetrical peak is characteristic of covalent bonding[11].

References

1. Shibata, H., Sakamoto, K., Ouchi, A. & Kurata, M. Chemical interaction between granular B_4C and 304L-type stainless steel materials used in BWRs in Japan. *J. Nucl. Sci. Technol. (Tokyo, Jpn.)*, DOI: 10.1080/00223131.2015.1011721.
2. Steinbrück, M. Influence of boron carbide on core degradation during severe accidents in LWRs. *Ann. Nucl. Energy* **64,** 43–49 (2014).
3. Zheng, X., Ishikawa, J., Itoh, H., Tamaki, H. & Maruyama, Y. Literature Review on Experiments and Models Associated with Degradation and Oxidation of Boron Carbide Control Material during Severe Accidents, *JAEA-Review* 2014–016, Japan Atomic Energy Agency, Tokai, Ibaraki, Japan (2014).
4. de Luze, O. Degradation and oxidation of B_4C control rod segments at high temperatures. A review and code interpretation of the BECARRE program. *Nucl. Eng. Des.* **259,** 150–165 (2013).
5. Hofmann, P. Markiewicz, P. & Spino, J. Reaction behavior of B_4C absorber material with stainless steel and zircaloy in severe light water reactor accidents. *Nucl. Technol.* **90.2,** 226–244 (1990).
6. Iihara, J. *et al.* Element-Selective Observation of Electronic Structure Transition between Semiconducting and Metallic States in Boron-Doped Diamond Using Soft X-Ray Emission and Absorption Spectroscopy. *Jpn. J. Appl. Phys.* **44,** 6612–6617 (2005).
7. Hanafusa, A. *et al.* Local structure analysis of boron-doped graphite by soft X-ray emission and absorption spectroscopy using synchrotron radiation. *J. Appl. Phys.* **110,** 053504 (2011).
8. Terauchi, M. *et al.* Present State of TEM-SXES Analysis and its Application to SEM aiming Chemical Analysis of Bulk Materials. *Microsc. Microanal.* **20.S3,** 682–683 (2014).
9. Takahashi, H. *et al.* Exciting Possibilities of Soft X-ray Emission Spectroscopy as Chemical State Analysis in EPMA and FESEM. *Microsc. Microanal.* **20.S3,** 684–685 (2014).
10. Zschornack, G. H. *Handbook of X-Ray Data*, Springer Science & Business Media (2007).
11. Tanaka, K., Yoshino, M. & Suzuki, K. Soft X-Ray Emission Study of Chemical Bonding in Fe- and Ni-Metalloid Alloy Glasses. *J. Phys. Soc. of Japan* **51,** 3882–3887 (1982).
12. Muramatsu, Y., Oshima, M. & Kato, H. Resonant X-Ray Raman Scattering in B Kα Emission Spectra of Boron Oxide (B_2O_3) Excited by Undulator Radiation. *Phys. Rev. Lett.* **71,** 448–451 (1993).

Acknowledgements

The authors thank Hideyuki Takahashi, Hideki Matsui, Akihiko Kimura and Satoshi Konishi for fruitful discussion. EPMA-SXES experiments were performed in the frame of ADMRIE project, supported by the Ministry of Education, Culture, Sports, Science and Technology of Japan.

Author Contributions

R.K. proposed and designed the research, R.K. and Y.H. carried out the EPMA-SXES experiment and analyzed the data, R.K. wrote the manuscript, K.S. and T.H. performed the high-temperature steam oxidation experiment. All co-authors contributed to discussions.

Additional Information

Competing financial interests: The authors declare no competing financial interests.

How to cite this article: Kasada, R. *et al.* Chemical State Mapping of Degraded B_4C Control Rod Investigated with Soft X-ray Emission Spectrometer in Electron Probe Micro-analysis. *Sci. Rep.* **6**, 25700; doi: 10.1038/srep25700 (2016).